

# Evidence for gravitational lensing of GRB 200716C

Xing Yang<sup>1</sup>, Hou-Jun Lü<sup>1</sup>, Hao-Yu Yuan<sup>1</sup>, Zhao Zhang<sup>2</sup>, Bin-Bin Zhang<sup>2</sup>, and En-Wei Liang<sup>1</sup>

## ABSTRACT

Observationally, there are a small fraction GRBs prompt emission observed by Fermi/GBM that are composed of two pulses. Occasionally, the cosmological distance of GRB may be lensed when a high mass astrophysical object reside in path between GRB source and observer. In this paper, we are lucky to find out GRB 200716C with two-pulse emission which duration is a few seconds. We present a Bayesian analysis identifying gravitational lensing in both temporal and spectral properties, and calculate the time delay ( $\Delta t \sim 1.92$  s) and magnification ( $\gamma \sim 1.5$ ) between those two pulses based on the temporal fits. One can roughly estimate the lens mass is about  $2.38 \times 10^5 M_{\odot}$  in the rest frame. If the first pulse of this GRB near triggered time is indeed gravitationally echoed by a second pulse, GRB 200716C may be a short GRB candidate with extended emission.

*Subject headings:* Gamma-ray burst: general

## 1. Introduction

Theory of General Relativity (GR) predicts that the space is curved by the compact objects, and the phenomena arising from the deflection of electromagnetic radiation (light ray) toward the mass in a field of gravity are called gravitational lensing (Blandford & Narayan 1992). A point mass gravitational lensing magnifies and makes two different images of the source when a massive object is located close to the line of sight between an observer and a source (Treu 2010 for a review). The photons traveling a longer distance will arrive first, but shorter path traversing deeper into the gravitational potential of the lens will delay arrive due to the stronger time dilation. Thus, the gravitationally retarded image is dimmer than the first image (Section 2 in details). The observational signature of such effect is an initial pulse followed by a duplicate echoed. The duration of the time delay between those two emission depended on the mass of the gravitational lens and magnification of those two images (Mao 1992; Paynter et al. 2021). It predict that the profile of light curve for those two images should be similar even the different intensity of them. However, the gravitational

---

<sup>1</sup>Guangxi Key Laboratory for Relativistic Astrophysics, School of Physical Science and Technology, Guangxi University, Nanning 530004, China; lhj@gxu.edu.edu

<sup>2</sup>Key Laboratory of Modern Astronomy and Astrophysics (Nanjing University), Ministry of Education, Nanjing 210093, China

lensing does not change photon energies, it means that all source images should have the same spectra (Paczynski 1987; Mao 1992).

Gamma-ray Bursts (GRBs) are one of the extremely luminous events and active high-energy transients since it was discovered in 1963 (Kumar & Zhang 2015 for a review), and its spectroscopically measured redshifts span the range from 0.0085 (Galama et al. 1998; Kulkarni et al. 1998) to 9.4 (Cucchiara et al. 2011) within more than  $10^4$  observed GRBs. The discovery optical sources with redshifts of gravitationally lensed range from 0.102 to 5.699 (Kochanek et al. 2018), it means that the GRBs may be gravitationally lensed occasionally (Paczynski 1986). If this is the case, GRB plays an important role to search for the evidence of gravitational lensing, and each image with a gravitationally induced time delay and different magnification can be detected through the observed burst light curve (Paczynski 1986; Blandford & Narayan 1992; Kalantari et al. 2021). Based on the time delay and the ratio of peak flux during those two images, one can roughly estimate the lens mass in the rest frame (Mao 1992; Paynter et al. 2021; Kalantari et al. 2021).

From observational point of view, a small fraction of GRBs prompt emission observed by Fermi/GBM, are composed of two or more emission episodes with a quiescent time which may last up to  $\sim 100$  s in the rest frame (Koshut et al. 1995; Lazzati 2005; Burlon et al. 2008; Bernardini et al. 2013; Hu et al. 2014; Lan et al. 2018). More interestingly, Lan et al (2018) performed a systematic analysis of both spectral and temporal properties of the GRB prompt emission observed by Fermi/GBM, which show the two-episode emission components in the light curves with quiescent times of up to hundreds of second. Statistically speaking, they found that the spectral of those two-episode emission components are not significant difference, but they do not analyse carefully to the light curve of those two-episode components. Recently, Paynter et al (2021) claimed that they have found out a possible signature of a gravitational lens in the light curve of GRB 950830 with two-episode emission. It means that those two-episode emission are gravitationally-lensed images of the same single-episode source. However, they do not present more details of spectral for those two-episode emission.

One question is that whether we can search for robust signatures of gravitational lensing in GRB to produce two images within source-lens-observer geometry, and manifest in the both light curve and spectral. By systematically searching for GRBs observed by both Fermi/GBM and Swift/BAT, we are lucky to find out GRB 200716C with two-episode emission. Its temporal and spectral properties satisfy with requirements of the theoretical predictions of gravitational lensing. In this paper, we focus on discussing the evidence for gravitational lensing of GRB 200716C based on the observational data. In the §2, we show the basic theory of gravitational lensing. A comprehensively data reduction and analysis

of GRB 200716C are presented in §3. Conclusions are drawn in §4 with some additional discussion.

## 2. Basic theory of gravitational lensing

By considering a light ray from distant source to approach a point mass ( $M$ ), the bend angle  $\alpha$  in the geometrical optics is given as

$$\alpha = \frac{4GM}{c^2 b}, \quad (1)$$

where  $b$  is the impact parameter by denoting the distance of closest approach of the ray to the mass. Figure 1 is the cartoon picture of geometrical optics by a point mass. First, let us label the observer-source distance  $D_{\text{os}}$ , the observer-lens distance  $D_{\text{ol}}$ , and the lens-source distance  $D_{\text{ls}}$ . By assuming the weak-field and thin-lens approximation, one has  $\alpha = \frac{4GM}{c^2 b} \ll 1$  (i.e., ), and  $b \ll D_{\text{ol}}$ , implies  $\theta \ll 1$ . Since  $\beta < \theta$ ,  $\beta$  is also small angle. Based on mathematical geometry of projecting on vertical line for a small angle, we can write

$$D_{\text{ls}}\alpha + D_{\text{os}}\beta = D_{\text{os}}\theta \quad (2)$$

Combining Eq.(1) and Eq. (2), one can solve the quadratic equation for  $\theta$ , and find two solutions,

$$\theta_{\pm} = \frac{1}{2}[\beta \pm (\beta^2 + \frac{16GM}{c^2} \frac{D_{\text{ls}}}{D_{\text{ol}}D_{\text{os}}})^{1/2}] \quad (3)$$

For small angle, one multiplied by  $D_{\text{ol}}$  in both sides of Eq. (4) to solve  $b$ ,

$$b_{\pm} = \frac{1}{2}[\lambda \pm (\lambda^2 + \frac{16GM}{c^2} \frac{D_{\text{ls}}D_{\text{ol}}}{D_{\text{os}}})^{1/2}] \quad (4)$$

Thus, there will always be two lensed images for a point mass lens (Blandford & Kochanek 1987).

In order to find out the relationship between time delay ( $\Delta t$ ) and magnification ( $\gamma$ ) from the unlensed to lensed system, we define a critical radius (or called Einstein radius),

$$r_{\text{cr}} = (\frac{4GM}{c^2} \frac{D_{\text{ls}}D_{\text{ol}}}{D_{\text{os}}})^{1/2} \quad (5)$$

inside of which significant magnification takes place, because the lensing changes the cross section, but not the surface brightness (Turner et al. 1984). By defining a dimensionless impact parameter  $f = \lambda/r_{\text{cr}}$ , the Eq.(4) can become as

$$b_{\pm} = \frac{r_{\text{cr}}}{2}[f \pm \sqrt{f^2 + 4}]. \quad (6)$$

89 The magnification (or the ratio of fluxes of individual images) can be expressed as

$$\gamma = \frac{I_{b+}}{I_{b-}} = \frac{(f^2 + 2) + f\sqrt{f^2 + 4}}{(f^2 + 2) - f\sqrt{f^2 + 4}} \quad (7)$$

90 The time delay can be contributed by two effects when the arrival of photons followed with  
 91 two paths in Figure 1. One is geometric with different path lengths, and another one is the  
 92 experience different general relativistic time dilations of two rays when two paths traverse  
 93 different gravitational potentials (Weinberg 1972). Thus, the time delay can be given as

$$\Delta t = \frac{D_{ol}D_{ls}}{2D_{os}}(\alpha_-^2 - \alpha_+^2) + \frac{2GM_z}{c^3}\ln\left(\frac{b_+^2}{b_-^2}\right) \quad (8)$$

94 By invoking Eq. (7), one can re-write the time delay as

$$\begin{aligned} \Delta t &= \frac{2GM_z}{c^3} \left[ \frac{1}{2}f\sqrt{f^2 + 4} + \ln\left(\frac{f^2 + 2 + f\sqrt{f^2 + 4}}{f^2 + 21f\sqrt{f^2 + 4}}\right) \right] \\ &= \frac{2GM_z}{c^3} \left[ \frac{\gamma - 1}{\sqrt{\gamma}} + \ln(\gamma) \right] \end{aligned} \quad (9)$$

95 where  $M_z = M(1 + z)$  is the redshifted lens mass.

96 GRBs have a good temporal resolution in  $\gamma$ -ray band, and the time delay and magnifi-  
 97 cation between the two images can be observed by considering both difference in geometric  
 98 path and relative difference in gravitational field strength. So that it is easy to estimate the  
 99 mass of gravitational lensing,

$$M_z = \frac{c^3\Delta t}{2G} \left( \frac{\gamma - 1}{\gamma} + \ln(\gamma) \right)^{-1} \quad (10)$$

### 100 3. Data reduction and analysis

#### 101 3.1. Temporal analysing the prompt emission of GRB 200716C

102 GRB 200716C triggered Swift/Burst Alert Telescope (BAT), Insight-HXMT, and Fermi/Gamma-  
 103 ray Burst Monitor (GBM). Due to no public of Insight-HXMT data, in this section, we  
 104 only focus on analysing the prompt emission of GRB 200716C observed by Swift/BAT and  
 105 Fermi/GBM.

### 3.1.1. Swift data reduction

GRB 200716C triggered the BAT at 22:57:41 UT on 16 July 2020 (Ukwatta et al. 2020). We downloaded the BAT data from the *Swift* website<sup>1</sup>, and use the standard HEASOFT tools (version 6.28) to process the BAT data. More details of analysing, please refer to (Sakamoto et al. 2008; Zhang et al. 2009; Lü et al. 2020). The light curves in different energy bands are extracted with the time-bin size . Then, we calculate the cumulative distribution of the source counts using the arrival time 8 ms. The light curve shows two prominent peaks with duration about 5.3 s in 15-150 keV (see Figure 2), but the a weak activity is still visible until about 90 seconds.

The light curve of GRB prompt emission with pulses, is usually described with the fast-rise exponential-decay (FRED) model (Norris et al. 1996). In order to test the consistency of structure for those two pulses, we also employ the FRED model plus Gaussian function to fit the pulses of GRB 200716C. By invoking the public code from Paynter et al. (2021), we used the same method from Paynter et al. (2021) to fit the light curve<sup>2</sup>. Here, we adopt two approaches to fit the data. Firstly, we used the same parameters (except the peak time and normalization) of one FRED model to fit those two pulses, and obtain the values  $\ln(\mathcal{Z}_L)$ , if we believe they are from the gravitational lensing (called “FL”). Then, we used the one FRED model plus one Gaussian function to fit the same data, and obtain the values  $\ln(\mathcal{Z}_{LG})$  (called “FSL”). On the other hand, we also used two FRED models to fit those two pulses with different parameters to get the values  $\ln(\mathcal{Z}_{NL})$ , if they are independent between each other (called “FF”). At the same time, two FRED models plus two Gaussian function are invoked to fit the same data to get the values  $\ln(\mathcal{Z}_{NLG})$  (called “FS”). In order to determine which model is to prefer the data, we calculate the Bayesian evidence for each model with Bayesian factor ( $\ln(BF)$ ), which is defined as  $\ln(BF) = \max(\ln(\mathcal{Z}_L), \ln(\mathcal{Z}_{LG})) - \max(\ln(\mathcal{Z}_{NL}), \ln(\mathcal{Z}_{NLG}))$ . If the  $\ln(BF)$  is larger than 8, then, this is considered as strong evidence to support of one model over the other (Thrane & Talbot 2019; Paynter et al. 2021).

We separate the Swift/BAT light curves into four available broadband energy channels (see Section 4), and independently calculate the value of  $\ln(BF)$  in those four channels (see Table 1). We find that the values of  $\ln(BF)$  are between -0.1 and 7.0 in each channel, and the total  $\ln(BF)$  value from each of the channels is about 15.24 in favour of lensing hypothesis. This is strong statistical evidence to support for the lensing hypothesis.

---

<sup>1</sup><https://www.swift.ac.uk/archive/selectseq.php?tid=00982707&source=obs>

<sup>2</sup>More details of this method and public code, please refer to Paynter et al. (2021).

### 3.1.2. Fermi data reduction

At 22:57:41.18 UT on 16 July 2020, the GBM was triggered and located GRB 20716C (Veres et al. 2020). GBM has 12 sodium iodide (NaI) and two bismuth germanate (BGO) scintillation detectors are covering the energy range from 8 keV to 40 MeV (Meegan et al. 2009). We downloaded the corresponding Time-Tagged-Event data from the public data site of *Fermi*/GBM<sup>3</sup>. For more details of data reduction of light curve procedure refer to (Zhang et al. 2016). The light curves of n0 and b0 detectors with 8 ms and 64 ms time-bin are shown in Figure 3, it consists of two pulses with a duration 3.3 s in 50-300 keV. There is not significant weak emission after the second pulse in the GBM temporal analysis.

Similarly with the pulse fitting of Swift/BAT data, we also apply for fitting the Fermi/GBM data with FRED model plus Gaussian function. Here, we calculate the Bayes factor in four available energy channels (see Section 4) with 8 ms and 64 ms time-bin, respectively. For 8 ms time-bin, the values of  $\ln(BF)$  are between 0.5 and 9.0 in each channel (see Table 1), and the total  $\ln(BF)$  value from each of the channels is about 19.94 in favour of lensing hypothesis. But for 16 ms time-bin, the  $\ln(BF)$  is -0.5 during the first energy channel, other three channels are range from 4.0 to 9.0. The total  $\ln(BF)$  values from each of the channels is about 19.56, which is close to that value of  $\ln(BF)$  for 8 ms time-bin. It suggests that the total  $\ln(BF)$  value for each energy channels seems to be not dependent on the time resolution. At least, this is also strong statistical evidence to support for the lensing hypothesis.

## 3.2. Extracting and fitting the spectrum of GRB 200716C

We do not extract the spectrum of GRB 200716C observed BAT due to its narrow energy band, but focus on the wide energy band in GBM. We extract the time-averaged spectrum of first (time interval  $(-0.3 - 1.9)$  s) and second (time interval  $(1.9 - 4.1)$  s) pulses of GRB 200716C, respectively. The background spectra are extracted from the time intervals before and after the those two pulses and modeled with an empirical function (Zhang et al. 2011). The spectral fitting is performed by using Markov Chain Monte Carlo (MCMC) method with our automatic code “*McSpecfit*” in (Zhang et al. 2018). We adopted several spectral models which we usually selected to test the spectral fitting of burst, i.e., power-law (PL), cutoff power-law (CPL), Band function (Band), Blackbody (BB), as well as combinations of any two models. Then, we compare the goodness of the fits of those two pulses, respectively (see

---

<sup>3</sup><https://heasarc.gsfc.nasa.gov/FTP/fermi/data/gbm/triggers/>

Table 1). We find that the CPL model is the best one to adequately describe the observed data by invoking the Bayesian Information Criteria (BIC; Lü et al. 2017). The CPL model fit is shown in Figure 4, as well as parameter constraints of the fit<sup>4</sup>. For the first pulse, it gives peak energy  $E_{p,1} = (524 \pm 97)$  keV, and a lower energy spectral index of  $\alpha_1 = 0.96 \pm 0.05$ . For the second pulse, one has  $E_{p,2} = (566 \pm 164)$  keV, and  $\alpha_2 = 0.98 \pm 0.08$ . The best-fit parameters of CPL fits and other models are listed in Table 1.

The spectral properties of those two pulses are consistent with each other by using the CPL model within the error range. This is consistency of the prediction of lensing hypothesis. Based on above analysis, both light curve and spectral properties are in support of GRB 200716C from gravitational lensing.

#### 4. Time delay and magnification of GRB 200716C

The gravitational lensing does not change photon energies when its travel close to the compact objects, and it means that all wavelengths of light curve are equally affected by gravitational fields. In other words, firstly, the time delay of different pulses is independent of the photon energy, and it should be the same in different energy channels. Secondly, the gravitational magnification of each image is identical for every wavelength. In order to test this hypothesis with the observed data, we separate the Swift/BAT and Fermi/GBM light curves into four available broadband energy channels, respective<sup>5</sup>.

Based on the light curve fits for each energy channels and adopting similar method with Paynter et al. (2021), one can easy to calculate the time decay and magnification. For Swift/BAT data, we roughly calculate  $\Delta t \sim 1.93$  s and  $\gamma \sim 1.54$ . For 8 ms time-bin of Fermi/GBM data, one has  $\Delta t \sim 1.92$  s, and  $\gamma \sim 1.49$ . For 16 ms time resolution, one has  $\Delta t \sim 1.92$  s, and  $\gamma \sim 1.52$ . This indicate that both time delay and magnification are also independent on the time resolution. Figure 5 shows the ratio as function of energy channels of prompt emission which observed by Swift/BAt and Fermi/GBM (8ms and 64 ms time-bin), it seems to be consistent with each other for different energy channels and fiddereent time-bin. By invoking the Eq. (10), as well as adopting  $\Delta t \sim 1.92$  s and  $\gamma \sim 1.5$ , one can roughly estimate the lens mass in the rest frame is about  $2.38 \times 10^5 M_\odot$ . This is consistent

---

<sup>4</sup>Our spectral fitting results are different from Wang et al. (2021). The reason is possible of different time-interval selected.

<sup>5</sup>The light curve of Swift/BAT is divided into four energy channels as 15-25 keV, 25-50 keV, 50-100 keV, and 100-350 keV. The Fermi/GBM light curve is separated into 8-44 keV, 44-100 keV, 100-250 keV, and 250-900 keV.

with the result of Wang et al. (2021). There are several astrophysical objects during this mass range, such as globular clusters, dark matter, and black hole (Paynter et al. 2021). Here, we do not discuss more details for those potential objects.

## 5. Conclusion and discussion

GRB 200716C, is observed by *Swift*, *Fermi*, and Insight-HXMT with a few seconds duration. The prompt emission of this GRB consists of two pulses, and weak emission (called extended emission) lasting  $\sim 90$  s after the second pulse is visible in the *Swift*/BAT, but not significant in the *Fermi*/GBM temporal analysis. In this paper, we presented a comprehensive analysis of its temporal and spectral data, and try to test whether the first pulse of GRB 200716C near triggered time is indeed gravitationally echoed by a second pulse, indicating that both pulses are gravitationally-lensed images of the same single source pulse.

Firstly, we separate the Swift/BAT and Fermi/GBM light curves into four available broadband energy channels, respective, and the FRED model plus Gaussian function are invoked to fit the profile of two pulses in each channel by adopting the public code from Paynter et al. (2021). Then, we independently calculate the Bayesian evidence for each model with Bayesian factor ( $\ln(BF)$ ). We find that the total  $\ln(BF)$  value from each of the channels is about 19 for BAT and GBM (even with different time resolution). This value is much larger than 8, and is favoured with lensing hypothesis. It is also independent on the time resolution of prompt emission. Moreover, we also extract the spectral by using MCMC method with our automatic code “*McSpecfit*” in (Zhang et al. 2018). Several spectral models (PL, CPL, Band, and BB), or even combinations of any two models, are selected to fit. We find that the CPL model is the best one to adequately describe the observed data by comparing the goodness of the fits of those two pulses, respectively. Both  $E_p$  and  $\alpha$  values of those two pulses are consistent with each other within the error range. This is consistency of the prediction of lensing hypothesis, and is also strong statistical evidence to support for the lensing hypothesis of GRB 200716C.

Based on the light curve fits for each energy channels and adopting similar method with Paynter et al. (2021), we calculate the time decay and magnification of those two pulses with  $\Delta t \sim 1.92$  s and  $\gamma \sim 1.5$ . Those two values are also independent on the time resolution. The inferred lens mass is about  $2.38 \times 10^5 M_\odot$ , which mass range is consistent with several astrophysical objects, such as globular clusters, dark matter, and black hole (Paynter et al. 2021).

If the GRB 200716C in indeed the gravitational lensing, the total duration of prompt



emission of this GRB should be the duration of any one pulse. If this is the case, the GRB 200716C should be a typical short-duration GRB with extended emission. Wang et al. (2021) claim that the  $E_p - E_{\gamma, \text{iso}}$  of GRB 200716C is located in the population of typical short GRBs, even for individual pulse by assuming a POSSIBLE redshift  $z = 0.348$ . At least for this case, due to lack accurately information of host galaxy, we only can find out some indirectly evidence for gravitational lensing of GRB 200716C. The Smoking gun of gravitational lensing with GRB is not only the consistency of temporal and spectral with prediction of gravitational lensing, as well as some empirical relations, indeed accurately information of its host galaxy with two images. With the improvement of detection technology, we encourage to observers by invoking a large optical telescopes to followup, especially, for those GRBs with two-pulse emission in the future.

We acknowledge the use of the public data from the *Swift* data and *Fermi* data archive. This work is supported by the National Natural Science Foundation of China (grant No. 11922301), the Guangxi Science Foundation (grant Nos. 2017GXNSFFA198008, and AD17129006), the Program of Bagui Young Scholars Program (LHJ), and special funding for Guangxi distinguished professors (Bagui Yingcai and Bagui Xuezhe).

## REFERENCES

- Bernardini, M. G., Campana, S., Ghisellini, G., et al. 2013, *ApJ*, 775, 67. doi:10.1088/0004-637X/775/1/67
- Blandford, R. D. & Narayan, R. 1992, *ARA&A*, 30, 311. doi:10.1146/annurev.astro.30.1.311
- Blandford, R. D. & Kundic, T. 1997, *The Extragalactic Distance Scale*, 60
- Burlon, D., Ghirlanda, G., Ghisellini, G., et al. 2008, *ApJ*, 685, L19. doi:10.1086/592350
- Cucchiara, A., Levan, A. J., Fox, D. B., et al. 2011, *ApJ*, 736, 7. doi:10.1088/0004-637X/736/1/7
- Galama, T. J., Vreeswijk, P. M., van Paradijs, J., et al. 1998, *Nature*, 395, 670. doi:10.1038/27150
- Hu, Y.-D., Liang, E.-W., Xi, S.-Q., et al. 2014, *ApJ*, 789, 145. doi:10.1088/0004-637X/789/2/145
- Kalantari, Z., Ibrahim, A., Rahimi Tabar, M. R., et al. 2021, arXiv:2105.00585

- 258 Koshut, T. M., Kouveliotou, C., Paciesas, W. S., et al. 1995, *ApJ*, 452, 145.  
259 doi:10.1086/176286
- 260 Kulkarni, S. R., Frail, D. A., Wieringa, M. H., et al. 1998, *Nature*, 395, 663.  
261 doi:10.1038/27139
- 262 Kumar, P. & Zhang, B. 2015, *Phys. Rep.*, 561, 1. doi:10.1016/j.physrep.2014.09.008
- 263 Lan, L., Lü, H.-J., Zhong, S.-Q., et al. 2018, *ApJ*, 862, 155. doi:10.3847/1538-4357/aacda6
- 264 Lazzati, D. 2005, *MNRAS*, 357, 722. doi:10.1111/j.1365-2966.2005.08687.x
- 265 Lü, H.-J., Yuan, Y., Lan, L., et al. 2020, *ApJ*, 898, L6. doi:10.3847/2041-8213/aba1ed
- 266 Lü, H.-J., Lü, J., Zhong, S.-Q., et al. 2017, *ApJ*, 849, 71. doi:10.3847/1538-4357/aa8f99
- 267 Mao, S. 1992, *ApJ*, 389, L41. doi:10.1086/186344
- 268 Meegan, C., Lichti, G., Bhat, P. N., et al. 2009, *ApJ*, 702, 791. doi:10.1088/0004-  
269 637X/702/1/791
- 270 Paczynski, B. 1986, *ApJ*, 308, L43. doi:10.1086/184740
- 271 Paczynski, B. 1987, *ApJ*, 317, L51. doi:10.1086/184911
- 272 Paynter, J., Webster, R., & Thrane, E. 2021, *Nature Astronomy*, 5, 560. doi:10.1038/s41550-  
273 021-01307-1
- 274 Sakamoto, T., Barthelmy, S. D., Barbier, L., et al. 2008, *ApJS*, 175, 179. doi:10.1086/523646
- 275 Thrane, E. & Talbot, C. 2019, *PASA*, 36, e010. doi:10.1017/pasa.2019.2
- 276 Treu, T. 2010, *ARA&A*, 48, 87. doi:10.1146/annurev-astro-081309-130924
- 277 Ukwatta, T. N., Barthelmy, S. D., Beardmore, A. P., et al. 2020, GRB Coordinates Network,  
278 Circular Service, No. 28124, 28124
- 279 Veres, P., Meegan, C., & Fermi GBM Team 2020, GRB Coordinates Network, Circular  
280 Service, No. 28135, 28135
- 281 Wang, Y., Jiang, L., Ren, J., et al. 2021, arXiv:2107.10796
- 282 Weinberg, S. 1972, *Gravitation and Cosmology: Principles and Applications of the General*  
283 *Theory of Relativity*, by Steven Weinberg, pp. 688. ISBN 0-471-92567-5. Wiley-VCH  
284 , July 1972., 688

- 285 Zhang, B.-B., Zhang, B., Castro-Tirado, A. J., et al. 2018, *Nature Astronomy*, 2, 258.  
286 doi:10.1038/s41550-018-0387-2
- 287 Zhang, B.-B., Uhm, Z. L., Connaughton, V., et al. 2016, *ApJ*, 816, 72. doi:10.3847/0004-  
288 637X/816/2/72
- 289 Zhang, B.-B., Zhang, B., Liang, E.-W., et al. 2009, *ApJ*, 690, L10. doi:10.1088/0004-  
290 637X/690/1/L10
- 291 Zhang, B.-B., Zhang, B., Liang, E.-W., et al. 2011, *ApJ*, 730, 141. doi:10.1088/0004-  
292 637X/730/2/141

Table 1: The Bayes factor of fitting in different energy band observed by Swift/BAT and Fermi/GBM.

Instrument	Energy Channels	$\ln(\text{BF})$	model	$\ln(\mathcal{Z})$
Swift/BAT	(15-25) keV	-0.13	FL	-77.49 $\pm$ 0.32
			FF	-77.36 $\pm$ 0.33
	(25-50) keV	2.56	FL	-100.01 $\pm$ 0.40
			FF	-102.57 $\pm$ 0.44
	(50-100) keV	5.83	FL	-86.50 $\pm$ 0.40
			FF	-92.33 $\pm$ 0.49
	(100-350) keV	6.98	FL	-54.20 $\pm$ 0.38
			FF	-61.18 $\pm$ 0.42
Fermi/GBM (8 ms)	(8-44) keV	0.59	FL	-1326.21 $\pm$ 0.22
			FF	-1326.80 $\pm$ 0.25
	(44-100) keV	7.76	FL	-1121.57 $\pm$ 0.23
			FF	-1129.33 $\pm$ 0.26
	(100-250) keV	2.7	FL	-1158.81.21 $\pm$ 0.24
			FF	-1161.51 $\pm$ 0.27
	(250-1000) keV	8.89	FL	-872.57 $\pm$ 0.21
			FF	-881.46 $\pm$ 0.25
Fermi/GBM (16 ms)	(8-44) keV	-0.5	FL	-273.13 $\pm$ 0.22
			FF	-272.63 $\pm$ 0.24
	(44-100) keV	4.76	FL	-261.45 $\pm$ 0.23
			FF	-266.21 $\pm$ 0.26
	(100-250) keV	8.64	FL	-272.10 $\pm$ 0.23
			FF	-280.74 $\pm$ 0.27
	(250-1000) keV	6.66	FL	-216.33 $\pm$ 0.21
			FF	-222.99 $\pm$ 0.24

Table 2: Spectral fitting results of GRB 200716C with different models

Model	Pulse-1						Pulse-2					
	$\Gamma$	$\alpha$	$\beta$	$E_{p,1}$	kT	BIC	$\Gamma$	$\alpha$	$\beta$	$E_{p,2}$	kT	BIC
BB					$50 \pm 2$	774					$51.87 \pm 2.22$	728
CPL		$0.96 \pm 0.05$		$523 \pm 97$		342		$0.98 \pm 0.08$		$566 \pm 163$		529
CPL+BB		$1.02 \pm 0.16$		$306 \pm 98$	$128 \pm 2$	349		$0.56 \pm 0.29$		$320 \pm 122$	$9.13 \pm 1.43$	536
CPL+PL	$2.11 \pm 3.39$	$0.88 \pm 0.34$		$456 \pm 209$		353	$8.6415 \pm 24.23$	$0.98 \pm 0.47$		$576 \pm 350$		540
Band		$-0.96 \pm 0.05$	$-9.3 \pm 3804$	$522 \pm 97$		348		$-0.97 \pm 0.08$	$-8.5 \pm 5671$	$567 \pm 174$		535
Band+BB		$-0.95 \pm 0.06$	$-9.3 \pm 3802$	$518 \pm 101$	$0.84 \pm 2.42$	359		$-0.57 \pm 0.29$	$-6.8 \pm 617$	$325 \pm 125$	$9.14 \pm 1.43$	542
Band+PL	$9.34 \pm 28.8$	$-0.95 \pm 0.061$	$-9.3 \pm 3795$	$520 \pm 102$		359	$2.43 \pm 5.09$	$-0.97 \pm 0.077$	$-8.6 \pm 4907$	$562 \pm 184$		546

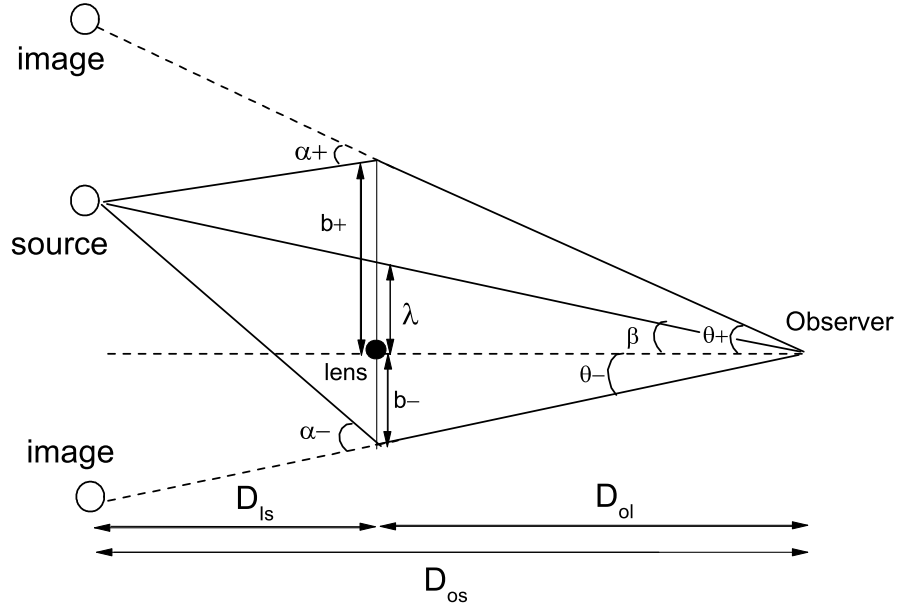


Fig. 1.— Cartoon picture of geometry of gravitational lensing

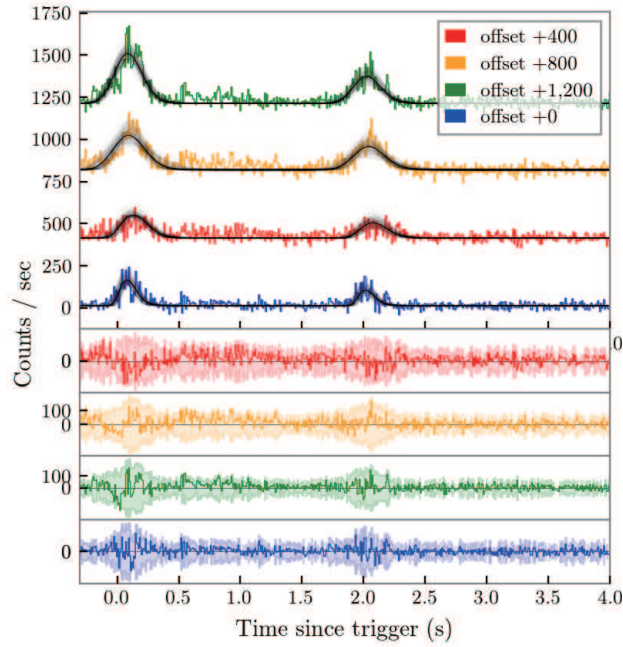


Fig. 2.— Light curve of prompt emission for gravitational lensed GRB 200716C observed by Swift/BAT. Different colour indicates different energy channel: red, (15-25) keV; yellow, (25-50) keV; green, (50-100) keV; blue, (100-350) keV. The solid black lines are the best fit with the empirical function (FRED), and the coloured shaded regions are the  $1\sigma$  standard statistical error.

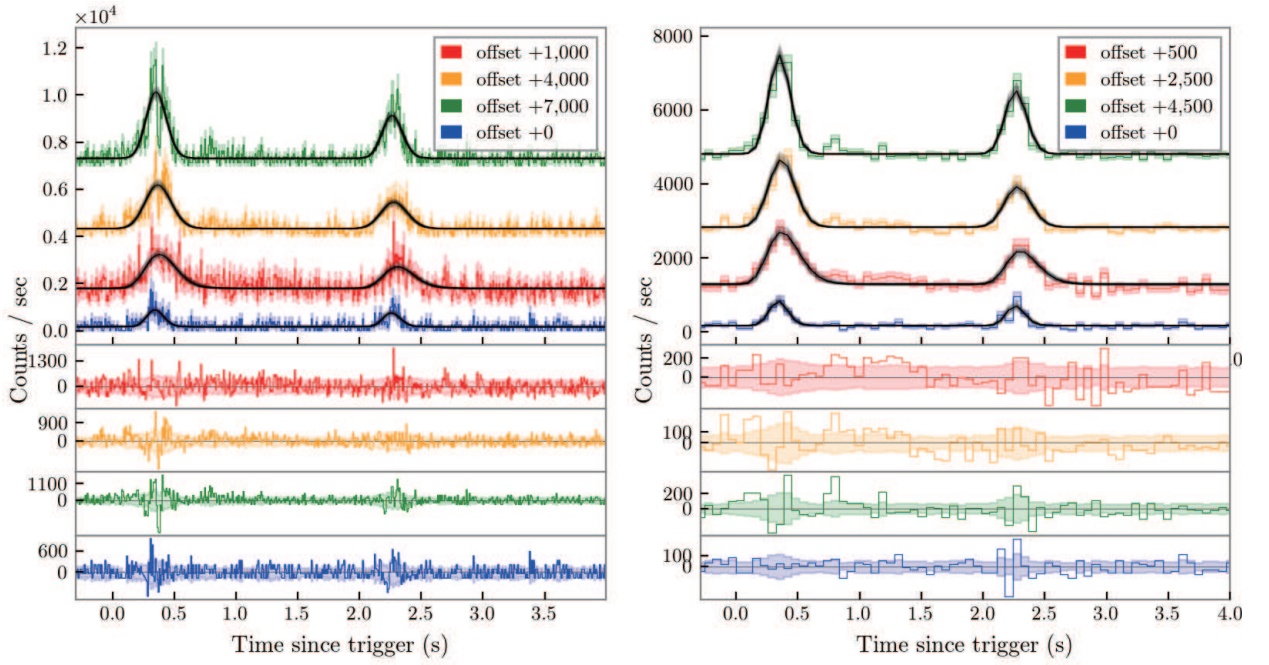


Fig. 3.— Similar with Figure 2, but observed by Fermi/GBM and different energy channel: red, (8-44) keV; yellow, (44-100) keV; green, (100-250) keV; blue, (250-900) keV. The left and right panels are the 8 ms and 64 ms time-bin, respectively.

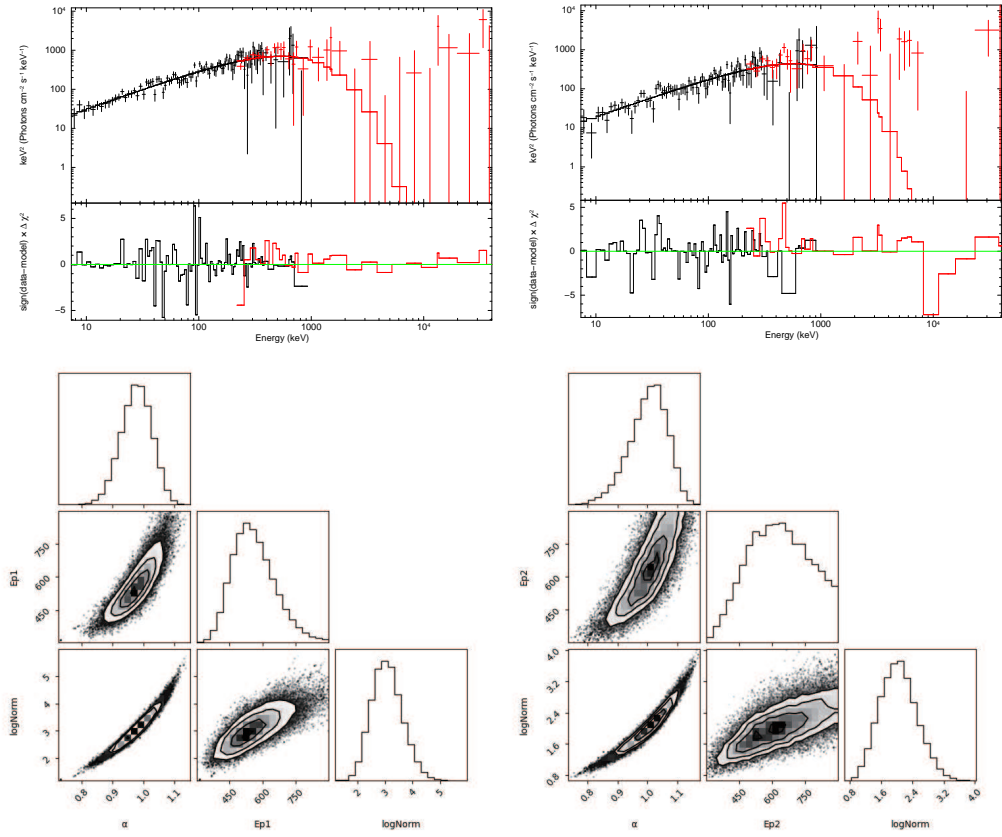


Fig. 4.— Spectral fits of GRB 200716C with the cutoff power-law model for Fermi/GBM. The  $\nu F_\nu$  spectrum and parameter constraints of the CPL fit for the first (left panels) and second pulses (right panels), respectively. Histograms and contours in the corner plots show the likelihood map of constrained parameters by using our McSpecFit package. The solid black circles are the  $1\sigma$ ,  $2\sigma$ , and  $3\sigma$  uncertainties, respectively.



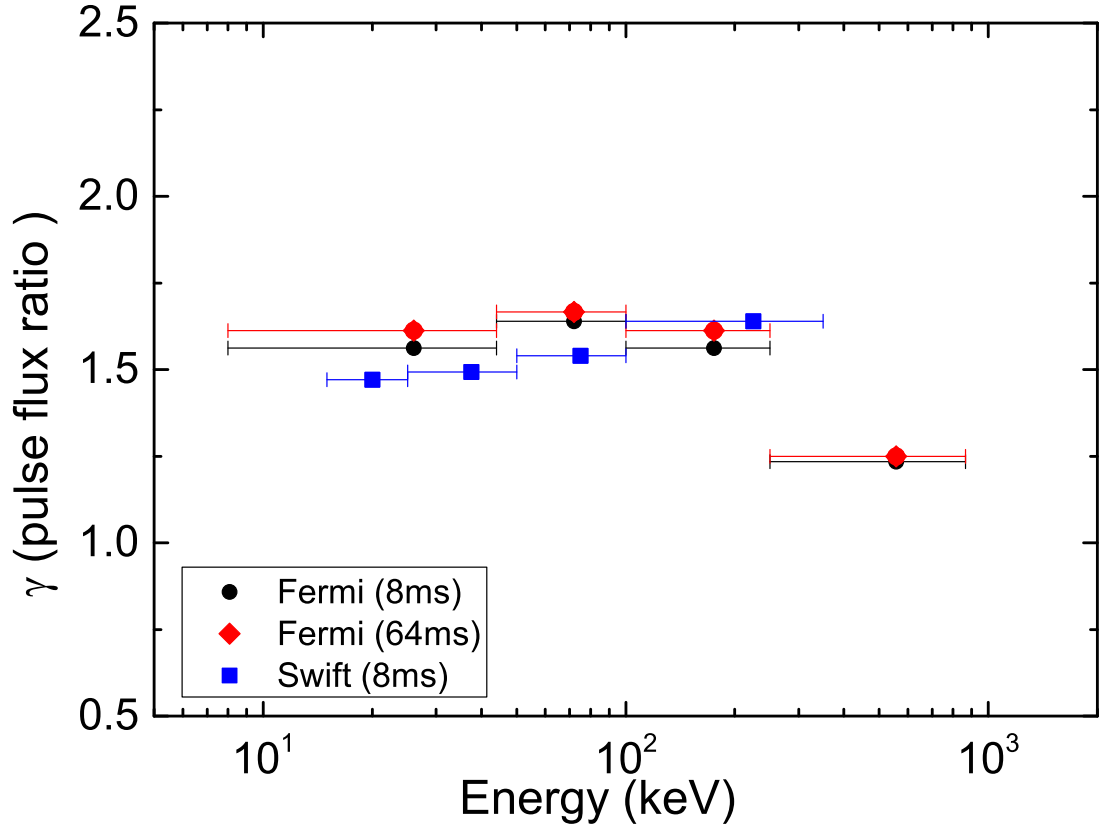


Fig. 5.— Peak flux ratio between those two pulses as function of energy channels for GRB 200716C.